Journal of Controlled Release 237 (2016) 71–77

Contents lists available at ScienceDirect

Journal of Controlled Release

journal homepage: www.elsevier.com/locate/jconrel

In situ growth of a C-terminal interferon-alpha conjugate of a phospholipid polymer that outperforms PEGASYS in cancer therapy

Jin Hu, Guilin Wang, Wenguo Zhao, Weiping Gao *

Department of Biomedical Engineering, School of Medicine, Tsinghua University, Beijing 100084, China

ARTICLE INFO

Article history:
Received 10 May 2016
Received in revised form 15 June 2016
Accepted 4 July 2016
Available online 5 July 2016

Keywords:
Interferon-alpha
Protein-polymer conjugate
Protein delivery
Atom transfer radical polymerization

ABSTRACT

Conjugating therapeutic proteins and peptides to poly(ethylene glycol) (PEG) can improve their pharmacokinetics and therapeutic potential. However, PEGylation suffers from non-specific conjugation, low yield and immunogenicity. Herein we report a new and general methodology to synthesize a protein-polymer conjugate with site-specificity, high yield and activity, long circulation half-life and excellent therapeutic efficacy. A phospholipid polymer, poly(2-methacryloyloxyethyl phosphorylcholine) (PMPC), was grown solely from the C-terminus of interferon-alpha to form a site-specific (C-terminal) and stoichiometric (1:1) PMPC conjugate of interferon-alpha in high yield. Notably, the PMPC conjugate showed 194- and 158-fold increases in systemic exposure and tumor uptake as compared with interferon-alpha, respectively. The *in vitro* antiproliferative bioactivity of the PMPC conjugate was 8.7-fold higher than that of PEGylated interferon-alpha (PEGASYS). In a murine cancer model, the PMPC conjugate completely inhibited tumor growth and cured 75% mice, whereas at the same dose, no mice treated with interferon-alpha or PEGASYS survived. We believe that this new approach to synthesize C-terminal protein conjugates of PMPC may be applicable to a large subset of protein and peptide drugs, thereby providing a general platform for the development of next-generation protein therapeutics.

1. Introduction

Therapeutic proteins and peptides have been widely used in clinical practice, but they have conspicuous limitations such as rapid clearance from the blood circulation, poor biocompatibility, high immunogenicity and low stability [1–3]. Covalent attachment of non-ionic, hydrophilic polyethylene glycol (PEG) to a protein, termed as PEGylation, is often used as a means to address the above shortcomings by increasing the size of the protein and providing a steric shield from the immune recognition, proteolysis and aggregation [4]. For instance, human interferon-alpha (IFN-α) has been widely used for the treatment of cancer and viral disease, but it exhibits short half-life ($t_{1/2}$ = 4–8 h) following systematic administration, resulting in frequent dosing and high systemic toxicity [5]. The pharmacokinetics of IFN-α can be enhanced *via* conjugating with 40 kDa branched PEG (PEGASYS, $t_{1/2}$ = 65 h) [6] or 20 kDa linear PEG (PEGINTRON, $t_{1/2}$ = 40 h) [7]. However, PEGylation is confronted with three major problems: 1) non-specific reaction of PEG with reactive amino acid residues randomly distributed on the protein scaffold leads to a heterogeneous mixture of positional isomers with reduced bioactivity, which further complicates the purification and separation procedures [8,9]; 2) the yield is quite low (<10%) since PEGylation involves the reaction between two large macromolecules [10]; 3) PEG itself is immunogenic, which can accelerate the blood clearance and alter the biodistribution after repeated injections of PEGylated drugs [11–13]. These shortcomings hamper the widespread application of PEGylation. Hence novel strategies that can circumvent these problems are of great interest.

In the past decade, *in situ* growth of a polymer from a protein (grafting from) has emerged as a potential alternative to direct conjugation of a polymer to a protein (grafting to) like PEGylation [14–21]. However, site-specific *in situ* growth (SIG) of a polymer from a protein to yield site-specific and stoichiometric protein-polymer conjugates in high yield with highly retained activity, significantly improved pharmacokinetics and therapeutic potential has remained a considerable challenge. To this end, we have recently demonstrated a general strategy for site-specific *in situ* growth (SIG) of a PEG-like polymer, poly(oligo(ethylene glycol) methyl ether methacrylate) (POEGMA), from the N-/C-terminus of model proteins, such as myoglobin (Mb), green fluorescence protein (GFP) and IFN-α to form site-specific (N-/C-terminal) and stoichiometric (1:1) POEGMA conjugates in high yield. The POEGMA conjugates showed retained activity and improved pharmacokinetics and therapeutic potential as compared with the native proteins [22–24]. However, as POEGMA is a kind of branched PEG, it can potentially induce an antibody response, which may neutralize the efficacy of POEGMA conjugates for chronic administration. Therefore, novel strategies that can circumvent this limitation are of interest.

We herein report a new and general strategy, SIG of a phospholipid polymer of poly(2-methacryloyloxyethyl phosphorylcholine) (PMPC), from a therapeutically important protein, IFN-α, to form a site-specific

* Corresponding author.
E-mail address: gaoweiping@tsinghua.edu.cn (W. Gao).

http://dx.doi.org/10.1016/j.jconrel.2016.07.007
0168-3659/

(C-terminal) and stoichiometric (1:1) PMPC conjugate of IFN-α (IFN-PMPC) (Fig. 1). The overall yield of the PMPC conjugate was as high as 63.4%, which was 70.4-fold higher than that (0.9%) of a similar IFN-PMPC conjugate prepared by post-polymerization conjugation (grafting to). The PMPC conjugate retained 53.6% *in vitro* antiproliferative bioactivity of native IFN-α, which was 8.7-fold higher than that (6.2%) of PEGASYS. The systemic exposure and tumor uptake of the PMPC conjugate were 194- and 158-fold higher than those of IFN-α, respectively, which were comparable to those of PEGASYS. More intriguingly, in a murine cancer model, the PMPC conjugate cured 75% mice, whereas at the same dose, no mice survive for over 49 and 63 days post administration with IFN-α and PEGASYS, respectively. These results show that a site-specific PMPC conjugate prepared by SIG can outperform PEGASYS that is the current gold standard for IFN-α delivery, which augurs well for its translation into the clinic. Herein, we call this strategy SIG of PMPC conjugates as an alternative to PEGylation.

We chose PMPC as a pharmacokinetically useful polymer instead of POEGMA for several reasons. First, PMPC is a biomimetic polymer with a phospholipid polar group, phosphorylcholine, in the side chain, which has excellent biocompatibility [25,26]. Second, PMPC is a zwitterionic polymer, which is resistant to non-specific protein adsorption from blood [27,28]. Third, PMPC is a Food and Drug Administration (FDA)-approved polymer, which has been used in the fields of medical devices and drug delivery [26,28]. These attributes make PMPC more interesting than PEG and POEGMA as a pharmacokinetically useful polymer.

Recently, IFN-α was conjugated to PMPC by non-specific post-polymerization conjugation to improve its pharmacokinetics [29], which, unfortunately, resulted in an unacceptable reduction in antiproliferative bioactivity (only 3.2% of bioactivity retention that is even lower than that (7%) of PEGASYS [7]) due to the non-specific nature of the conjugation. In contrast, this paper, for the first time, presents SIG of a site-specific PMPC conjugate of IFN-α and a head-to-head comparison of the site-specific PMPC conjugate with PEGASYS, which goes far beyond the preliminary pharmacokinetic result previously reported for the non-specific PMPC conjugate [29]. Such a direct comparison of a new delivery system with the clinical gold standard formulation is highly desired as it strongly questions the clinical utility of the new delivery system in the preclinical pipeline.

2. Materials and methods

2.1. Materials

All chemical reagents were purchased from Sigma Aldrich or J&K Scientific. All molecular biology reagents were purchased from New England Biolabs. All cell culture reagents and media were purchased from Gibco or Hyclone. All reagents were used as received, unless otherwise specified. Human Burkitt's B lymphoma cells (Daudi B) and human ovarian carcinoma cells (OVCAR-3) were purchased from cell bank of Chinese Academy of Medical Sciences. Female BALB/c nude mice were purchased from Vital River Laboratories (Beijing, China) and accommodated in animal research facility of Tsinghua University.

2.2. In situ ATRP of MPC from the C-terminus of IFN-α

IFN-α and IFN-Br were prepared according to our previous work [24]. *In situ* ATRP of MPC from the C-terminus of IFN-α was carried out in PBS buffer with an ice-water bath. A deoxygenated mixture of 5 μmol CuCl, 15 μmol $CuCl_2$, and 25 μmol 1,1,4,7,10,10-hexamethyltriethylenetetramine (HMTETA) dissolved in water was transferred into 4 mL of 50 μM deoxygenated IFN-Br solution and 800 μmol 2-methacryloyloxyethyl phosphorylcholine (MPC) in 10 mM PBS, 10% glycerol, pH 7.4 *via* a cannula transfer. The polymerization was allowed to react for 1.5 h under nitrogen atmosphere and stopped by exposing to air. The IFN-PMPC conjugates were separated from the reaction mixtures *via* desalting and AEX chromatography as described above. In a control experiment, IFN-α was used as an initiator for ATRP under the same reaction condition as was used for IFN-Br. The concentration of IFN-PMPC was quantified by BCA assay according to the instructions of BCA kit (Beyotime Biotech), using bovine serum albumin as the protein standard.

2.3. Post-polymerization conjugation for IFN-PMPC

As a control, IFN-PMPC was synthesized *via* post-polymerization conjugation, which includes two parts: the synthesis of PMPC and grafting PMPC to the C-terminus of IFN-α. In the first part, AEBM, instead of IFN-Br was used as an initiator for ATRP to synthesize PMPC as described above, followed by ultrafiltration to remove small soluble impurities. In the second part, in order to conjugate PMPC to the C-terminus of IFN-α, 25 μM IFN-$LPETGH_6$, 12.5 μM SrtA and 500 μM PMPC was mixed and incubated in a reaction buffer containing 50 mM Tris·HCl, 150 mM NaCl, 10 mM $CaCl_2$, pH 7.4. After an overnight incubation at 25 °C, SrtA was removed by cation exchange chromatography using an equilibration buffer of 20 mM Tris·HCl, pH 7.0 and an elution buffer of 20 mM Tris·HCl, 1 M NaCl, pH 7.0. After that, unreacted IFN-$LPETGH_6$ and PMPC were removed by anion exchange chromatography using an equilibration buffer of 20 mM Tris·HCl, pH 8.0 and an elution buffer of 20 mM Tris·HCl, 1 M NaCl, pH 8.0.

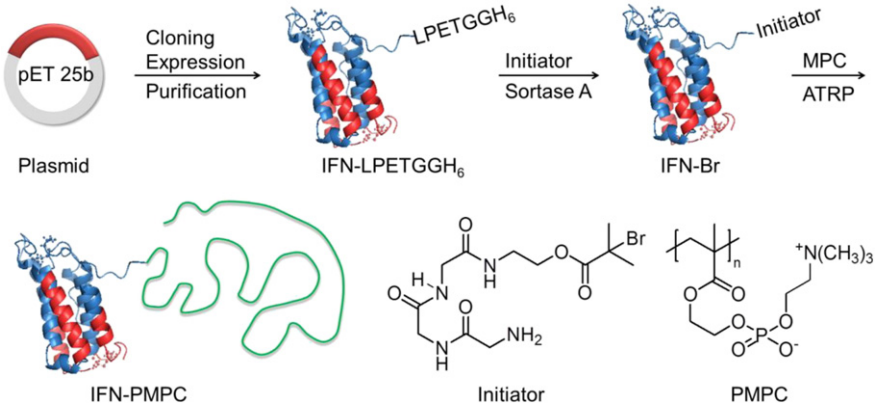

Fig. 1. Schematic illustration of site-specific *in situ* growth of PMPC from the C-terminus of IFN-α. First, a triglycine-functionalized atom transfer radical polymerization (ATRP) initiator (AEBM) is selectively attached to the C-terminus of IFN-α by sortase A catalyzed ligation to yield a macroinitiator (IFN-Br). Second, PMPC is site-specifically grown from IFN-Br *via* ATRP, producing an IFN-PMPC conjugate. The crystal structure of IFN-α was generated from PDB code 1ITF [30]. Receptor binding domains colored in red are distant from the C-terminus of IFN-α.

2.4. Physicochemical characterization

2.4.1. Gel permeation chromatography (GPC)

The IFN-PMPC conjugates were analyzed on a Waters HPLC/GPC system equipped with a UV detector (Waters 2489) operated at 280 nm and a refractive index detector (Waters 2414). Samples were separated by an Asahipak GS-520 HQ column (with a guard column) at the flow rate of 0.5 mL/min at 25 °C. The mobile phase consisted of 50 mM Tris·HCl, 150 mM NaCl, pH 7.4. A calibration curve was created by using PEG standards with different molecular weights for estimating the relative molecular weight of the IFN-PMPC conjugate. To characterize the molecular weight of PMPC, the IFN-PMPC conjugate (1 mg/mL) was incubated with proteinase K (0.5 mg/mL) in digestion buffer (50 mM Tris·HCl, 2 mM $CaCl_2$, pH 7.4) at 45 °C for 12 h to remove IFN before analysis. All the results were analyzed with Breeze 2 software.

2.4.2. Proton nuclear magnetic resonance (^{1}H NMR) spectroscopy

The ^{1}H NMR spectra were analyzed on a JEOL ECX-400 spectrometer, operating at 400 MHz, 25 °C with residual solvent as internal standard. The samples were freeze-dried and then dissolved into deuterium oxide before analysis.

2.4.3. Circular dichroism (CD)

CD spectra were carried out on a Pistar π-180 (Applied Photophysics Ltd) instrument with a far UV region between 190 nm and 260 nm. Samples were diluted to a concentration of 0.15 mg/mL in H_2O.

2.4.4. Inductively coupled plasma-optical emission spectrometry (ICP-OES)

The copper concentration of purified IFN-PMPC was recorded on ICP-OES (Varian Vista-Pro, Australia) using methods APAT CNR IRSA 3020 Man 29 2003. Samples were diluted to a concentration of 0.2 mg/mL in 25% aqua regia before analysis.

2.4.5. Dynamic light scattering (DLS)

DLS analysis was performed on a Malvern Zetasizer Nano-zs90 with a laser wavelength of 633 nm and a scattering angle of 90° at 25 °C. Samples were filtered (filter with 0.22 μm pore size, Millipore Corp.) before analysis. Data were analyzed using Zetasizer software 6.32.

2.5. In vitro cytotoxicity

The protocols of *in vitro* anti-tumor activity assessment were employed as described previously [24] with minor modifications. Daudi B cells were cultured in RPMI-1640 medium supplemented with 15% (vol/vol) fetal bovine serum (FBS) and 1% penicillin/streptomycin (Hyclone) at 37 °C in a humidified, 5% CO_2 atmosphere. 50 μL of 7500 cells were seeded per well in a 96-well plate (Corning). 50 μL of fresh medium containing serial IFN-α equivalent concentration of samples (2, 4, 10, 20, 100, 200, 600, 2000 and 20,000 pg/mL) were added to the corresponding wells. Wells filled with media and media-treated cells only were considered as background and control, defined as 0% and 100% cell viability, respectively. After incubating the plate for 4 d, the cell proliferation inhibition was measured by MTT assay according to the instructions of Cell Proliferation Assay kit (Promega). The data fitting and IC_{50} calculation were analyzed by GraphPad Prism 5.0 software and the results were presented as mean ± S.D.

2.6. In vivo study

The Laboratory Animal Facility at the Tsinghua University is accredited by AAALAC (Association for Assessment and Accreditation of Laboratory Animal Care International), and all animal protocols used in this study are approved by the Institutional Animal Care and Use Committee (IACUC).

2.6.1. Pharmacokinetics

The protocols of *in vivo* study (pharmacokinetics, biodistribution, *in vivo* anti-tumor evaluation and *in vivo* toxicity examination) were employed as previously described with minor modifications [24]. 9 female BALB/c nude mice (6-week old) were randomly distributed into three groups (n = 3 per group) and injected intravenously with IFN-α, PEGASYS, or IFN-PMPC at a dose of 1 mg IFN-α equivalent/kg body weight *via* tail veil. At desired time points (1, 5, 15, 30 min, 1, 3, 6, 24, 48, 72 and 96 h), blood samples (10 μL) were drawn from mice *via* tail vein into heparin anticoagulant tubes. After standing for 30 min at 4 °C, samples were centrifuged at 4000 ×g for 20 min, and plasma were isolated and stored at −80 °C. The concentration of IFN-α was determined by ELISA assay according to the directions of human IFN-α2 ELISA kit (PBL Interferon Source). Pharmacokinetic parameters were analyzed by DAS 3.0 software and fitted with a two-compartment model.

2.6.2. Biodistribution

The human ovarian carcinoma cell line OVCAR-3 was cultured in RPMI-1640 Medium containing 20% fetal bovine serum, 0.01 mg/mL bovine insulin and 1% penicillin/streptomycin. Female BALB/c nude mice (6-week old) were s.c. implanted in the left flank with 5×10^6 OVCAR-3 cells suspended in 0.1 mL mixture of serum free media/Matrigel (1:1) (BD Biosciences).When the tumor size reached 100–150 mm^3, mice were randomly assigned to three groups (n = 3 for each group) and i.v. administered IFN-α, PEGASYS and IFN-PMPC at a dosage of 1 mg IFN-α Equiv/kg body weight. At 2 h, 24 h and 96 h post injection, mice were immediately sacrificed and major organs (tumor, heart, kidney, liver, spleen, lung, pancreas, stomach, muscle and intestine) were collected, washed, dried, weighed and homogenized with an addition of 10 mM PBS extraction buffer (including 1 mM EDTA, 1 mM PMSF, 1% Triton X-100, 0.5% sodium deoxycholate and 1% phosphatase inhibitor cocktail). The quantification of IFN-α in tissue was the same as described above. The background of tissues from untreated mice was subtracted correspondingly. The data were displayed as percentage of total injected dose (%ID) per gram of tissue.

2.6.3. In vivo antitumor efficacy

The antitumor efficacy of IFN-PMPC conjugate was also evaluated in female BALB/c nude mice bearing OVCAR-3 tumor. Treatment started at three weeks post inoculation, at which time the tumors had been established (~20 mm^3). The mice were randomized into four test groups (n = 6 or 8 per group) and injected weekly with saline, IFN-α, PEGASYS or IFN-PMPC at a dose of 20 μg IFN equivalent/mouse until all the mice of control groups (the group of saline, IFN-α and PEGASYS) were sacrificed. Tumor volumes and body weights of the mice were monitored twice a week during the experimental period. The tumor volume was calculated using the formula: (width × width) × length) / 2. Mice would be sacrificed if their tumor size grew up to 500 mm^3 or weight loss was >15% of its initial weight. Statistical analysis was performed using GraphPad Prism software 5.0.

2.6.4. In vivo toxicity

To evaluate the *in vivo* toxicity of IFN-PMPC, histomorphology, clinical biochemistry and hematology of mice were assayed. After treatment with saline, IFN-α, PEGASYS or IFN-PMPC once a week, mice were sacrificed at day 21 after being treated for twice. Organs including tumors, hearts, livers and kidneys were collected, fixed with 4% neutral paraformaldehyde, embedded in paraffin, sliced up into 5 μm thick sections, mounted onto glass slides and stained with hematoxylin-eosin according to standard procedures. The photographs of all sections were imaged with a Nikon Eclipse 90i.

Blood was collected from retro-orbital sinus of the mice after being treated for five times (at day 42). Clinical biochemistry analysis of serum, including lactate dehydrogenase (LDH), creatine kinase isoenzymes (CK-MB), aspartate aminotransferase (AST), alanine aminotransferase (ALT), creatinine (CRE) and blood urea nitrogen (BUN) was

analyzed by Automatic Biochemical Analyzer (HITACHI). Hematological parameters of complete blood, including numeration of white blood cells (WBC), red blood cells (RBC), platelets (PLT) and the concentration of hemoglobin (HGB), was recorded on a Hematology Analyzer (SYSMEX).

2.7. Statistical analysis

Values were represented as mean ± standard deviation (S.D.). Statistical analysis were performed with GraphPad Prism software 5.0. Cumulative survival were analyzed by Log-rank (Mantel-Cox) test. The other data comparisons were carried out using Student's *t*-test. Differences were considered to be significant when the *P* value was <0.05.

3. Results and discussion

3.1. Synthesis and in vitro characterization of IFN-PMPC

The ATRP initiator (AEBM) was quantitatively, stoichiometrically and specifically attached to the C-terminus of IFN-α, by sortase-mediated protein ligation, to yield the macroinitiator IFN-Br [24]. ATRP of MPC from IFN-Br was performed in phosphate buffered saline (PBS) in an ice-water bath. At the end of the ATRP reaction, the ATRP solution was directly characterized by gel permeation chromatography (GPC) with a UV detector operated at 280 nm (Fig. 2a). The GPC trace of IFN-Br showed a relatively narrow peak at an elution time of 19.5 min, which coincided with that of IFN-LPETGGH$_6$, as expected. After the polymerization, the GPC peak for IFN-Br substantially decreased in intensity while a new peak at a shorter elution time of 13.8 min appeared, indicating the formation of an IFN-PMPC conjugate with a high MW. Integration of the peak areas of the IFN-Br and IFN-PMPC conjugates showed that the conversion of IFN-Br into IFN-PMPC was >90%, indicating the high initiation efficiency of ATRP of MPC from IFN-Br. S.D.S-PAGE also showed that the band for IFN-Br almost disappeared after the polymerization, accompanied by the emergence of a new band corresponding to the synthesized IFN-PMPC conjugate with a high MW (Fig. S1). In a control experiment in which IFN-α, instead of IFN-Br, was used as an initiator for ATRP of MPC at the same conditions as described in the ATRP of MPC from IFN-Br. As expected, ATRP of MPC did not occur without the ATRP initiator attachment of IFN-α (Fig. S2). Taken together, these results indicate the successful *in situ* growth of PMPC from the C-terminus of IFN-α by ATRP with high initiation efficiency.

Subsequently, the polymerization mixture was purified by anion exchange (AEX) chromatography to remove unreacted IFN-Br, followed by GPC analysis (Fig. 2a). After the purification, the GPC peak for unreacted IFN-Br disappeared, and only a peak corresponding to IFN-PMPC was observed, indicating the successful purification of the conjugate. After digestion of the conjugate with proteinase K to remove IFN (Fig. S3), the MW of the polymer was determined to be 57 kDa with a molar-mass dispersity ($Đ_M$) of 1.43 by GPC calibrated with PEG standards, which is similar to that of POEGMA of the IFN-POEGMA conjugate reported in our previous work [24]. Proton nuclear magnetic resonance (^{1}H NMR) further confirmed the synthesis of PMPC from IFN-Br (Fig. S4). The overall yield of the conjugate after the two-step reactions was determined to be about 63.4%, which was over 70.4-fold higher than that (0.9%) of an IFN-PMPC analogue with a similar MW synthesized by post-polymerization conjugation (Fig. S5). These data indicate that the SIG methodology is much more efficient than the conventional post-polymerization conjugation technique in synthesis of a site-specific and stoichiometric IFN-PMPC conjugate.

Circular dichroism (CD) spectroscopy showed that the highly α-helical structure of IFN-α was well preserved during the C-terminal modification process (Fig. 2b), suggesting that the SIG of PMPC seldom perturbed the secondary structure of IFN-α. The copper concentration of the purified IFN-PMPC solution was measured by inductively coupled plasma-optical emission spectrometry (ICP-OES) to be as low as 0.01 ppm, suggesting that the copper from the ATRP catalyst was successfully removed from the conjugate. Dynamic light scattering (DLS) showed that the hydrodynamic radius (R_h) of IFN-PMPC was 9.7 nm, which was nearly 5-fold larger than that of IFN-LPETGGH$_6$ (2.4 nm), IFN-Br (2.3 nm) or IFN-α (2.3 nm) (Fig. 2c), suggesting a prolonged circulation time of IFN-PMPC over IFN-α.

IFN-α is a highly pleiotropic cytokine with potent antiproliferative, immunoregulatory and antiviral properties [31,32]. We herein evaluated the *in vitro* antiproliferative activity of IFN-PMPC using a human Burkitt's B cell lymphoma line (Daudi B) (Fig. 2d). IFN-LPETGGH$_6$, IFN-Br and IFN-α showed similar bioactivities with half maximal inhibitory concentrations (IC_{50}'s) of 10.78, 11.18 and 10.77 pg/mL, respectively, indicating

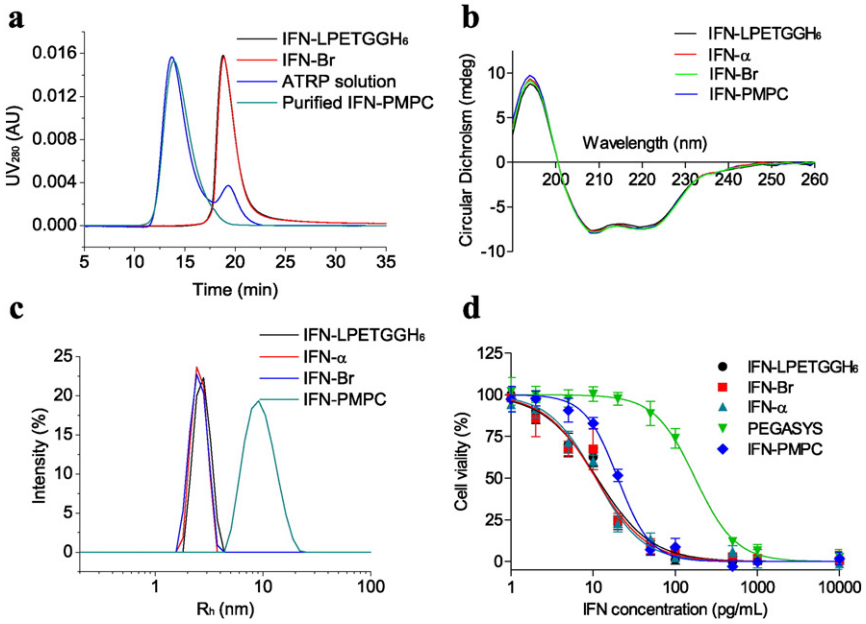

Fig. 2. Physicochemical characterization and *in vitro* bioactivity of IFN-PMPC. (a) GPC traces of the ATRP reaction solution and the purified IFN-PMPC conjugate. (b) CD spectra of IFN-LPETGGH$_6$, IFN-Br, IFN-α and IFN-PMPC. (c) DLS analysis of IFN-PMPC, where R_h is hydrodynamic radius. (d) *In vitro* cytotoxicity of IFN-PMPC against Daudi B. Data are shown as mean ± S.D. (n = 3).

that the tag fusion and ATRP initiator attachment to the C-terminus of IFN-α did not affect the biological activity. IFN-PMPC showed an excellent bioactivity retention of 53.6% (IC_{50} = 20.02 pg/mL) that was 8.7-fold greater than that (6.2%) of PEGASYS (IC_{50} = 175.00 pg/mL), indicating that SIG of a PMPC conjugate at the C-terminus of IFN-α is much better than non-specific PEGylation of IFN-α in *in vitro* bioactivity retention.

3.2. Pharmacokinetics and biodistribution

Encouraged by the promising *in vitro* properties of IFN-PMPC, we further evaluated the *in vivo* properties of IFN-PMPC in mouse models. At first, we assessed the pharmacokinetic behavior of IFN-PMPC following an intravenous injection in a nude mouse model. The data were fitted with a two-compartment pharmacokinetic model (Fig. 3a and Table S1). Unmodified IFN-α was quickly cleared from blood and was almost undetectable within 24 h. On the contrary, IFN-PMPC displayed a much slower clearance, and the plasma level (5.8×10^5 pg/mL) was 2140-fold higher than that of IFN-α (2.7×10^2 pg/mL) at 24 h post administration. The distribution ($t_{1/2\alpha}$) and terminal ($t_{1/2\beta}$) half-lives were 2.0 h and 51.6 h, respectively, which were 6.2-fold and 34.6-fold longer than those of IFN-α ($t_{1/2\alpha}$ = 0.33 h, $t_{1/2\beta}$ = 1.49 h), respectively. Notably, the level of systemic exposure ($AUC_{0-\infty}$) was increased by over 194-fold from 0.49 mg/mL h for IFN-α to 95.12 mg/mL h for IFN-PMPC. These results indicate that SIG of a PMPC conjugate can significantly improve the pharmacokinetics of IFN-α. In addition, the pharmacokinetic parameters of IFN-PMPC were comparable to those of PEGASYS, suggesting that a site-specific PMPC conjugate synthesized by SIG is equal to a non-specific PEG conjugate synthesized by conventional post-polymerization conjugation in improvement of the pharmacokinetics of IFN-α.

We further examined the biodistribution of IFN-PMPC in a murine model (bearing ovarian tumors with a size of 100–150 mm^3). At 2 h, 24 h and 96 h post injection, major tissues (tumor, heart, kidney, liver, spleen, lung, pancreas, stomach, muscle and intestine) were collected for the quantification of IFN-α in the tissues. Both IFN-PMPC and PEGASYS showed much greater accumulation in these major tissues than IFN-α (Fig. 3b and Fig. S6), due to their substantially better pharmacokinetics than IFN-α. Particularly, the level of IFN-PMPC (1.45×10^5 pg/g tissue) in the tumors was 158-fold higher that of IFN-α (9.16×10^2 pg/g tissue) at 24 h post administration, which was comparable to that (1.53×10^5 pg/g tissue) of PEGASYS (Fig. 3b). These results demonstrate that a site-specific PMPC conjugate prepared by SIG is similar to a non-specific PEG conjugate prepared by conventional PEGylation in improving the biodistribution of IFN-α.

3.3. In vivo antitumor activity and biological safety

Next, we evaluated the *in vivo* antitumor activity of IFN-PMPC in an OVCAR-3 xenograft model (Fig. 4). When the tumor size reached ~20 mm^3, mice were intravenously administered with saline, IFN-α, PEGASYS or IFN-PMPC once a week at a dosage of 20 μg IFN equivalent/mouse *via* tail vein until all the mice of control groups (the groups of saline, IFN-α and PEGASYS) were sacrificed. As expected, IFN-α at this dose was almost ineffective in inhibiting tumor growth as compared with saline (Fig. 4a). PEGASYS significantly inhibited tumor growth. In contrast, IFN-PMPC not only completely inhibited tumor growth but also eliminated the tumors. Notably, the tumors of six of eight mice treated with IFN-PMPC completely disappeared at 24 days post administration. At six weeks after the treatment, the average tumor size for IFN-PMPC was 16.0 mm^3, which was 33.7-, 29.3- and 14.1-fold smaller than those for saline (539.8 mm^3), IFN-α (468.2 mm^3) and PEGASYS (224.9 mm^3), respectively. These results indicate that IFN-PMPC outperforms PEGASYS and IFN-α in reducing tumor size, which correlated with a substantial increase in animal survival (Fig. 4b). The median survival time for mice treated with saline was 35 days, and treatment with IFN-α slightly increased this survival to 38 days. Treatment with PEGASYS further increased the survival to 63 days. In contrast, six of eight mice were tumor-free and alive for up to 180 days without any tumor recurrence and mouse death after the treatment with IFN-PMPC, and one of the rest mice held a small tumor of 64.0 mm^3 that did not grow up any more and the other was not sacrificed until day 93. The outperformance of IFN-PMPC over PEGASYS and IFN-α in anticancer efficacy was further confirmed by hematoxylin and eosin (H&E) staining of tumor tissue (Fig. 4c). The tumors of mice treated with saline consisted of typical, tightly packed tumor cells with morphological integrity, whereas the tumors of mice treated with IFN-α showed somewhat vacuolization and cell breakage, indicating the presence of tumor cell apoptosis. As expected, PEGASYS and IFN-PMPC treatments caused moderate and severe tumor cell apoptosis, respectively. Taken together, these results demonstrate that IFN-PMPC outperforms PEGASYS and IFN-α in cancer therapy, owing to the highly retained antiproliferative activity and significantly enhanced pharmacokinetics and tumor accumulation.

We finally evaluated the *in vivo* biological safety of IFN-PMPC by monitoring body weight change of the mice during the treatment and by histomorphology, clinical biochemistry and hematology assays. No body weight loss was observed for the mice treated with IFN-α, PEGASYS or IFN-PMPC (Fig. S7), suggesting that they were tolerable at this dose. No significant histological differences in major tissues, such as hearts, livers and kidneys, were observed between saline group and IFN-α, PEGASYS or IFN-PMPC groups (Fig. S8), indicating that these treatments did not induce noticeable damage to these major tissues. The clinical biochemical parameters related to liver, heart and kidney function markers of IFN-α, PEGASYS or IFN-PMPC treated mice were comparable to those of saline treated mice (Fig. S9), indicating that the treatment did not induced apparent liver, heart and kidney toxicity. Besides, the vital hematological markers of the mice treated with IFN-α,

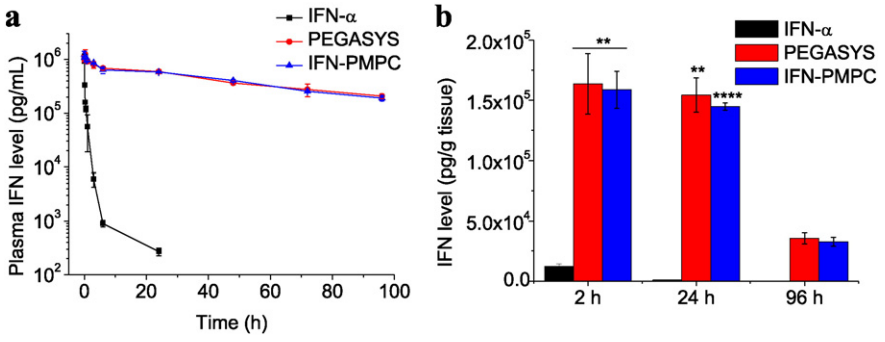

Fig. 3. Pharmacokinetics and tumor accumulation of IFN-PMPC. (a) Plasma concentrations of IFN-α, PEGASYS and IFN-PMPC as a function of time post administration (n = 3, $P < 0.001$ for IFN-PMPC and PEGASYS *versus* IFN-α). (b) Tumor concentrations of IFN-α, PEGASYS and IFN-PMPC at 2, 24 and 96 h post administration (n = 3, $^{**}P < 0.01$ for IFN-PMPC and PEGASYS *versus* IFN-α at 2 h post administration, $^{**}P < 0.01$ for PEGASYS *versus* IFN-α at 24 h post administration, $^{****}P < 0.0001$ for IFN-PMPC *versus* IFN-α at 24 h post administration). Data are shown as mean ± S.D.

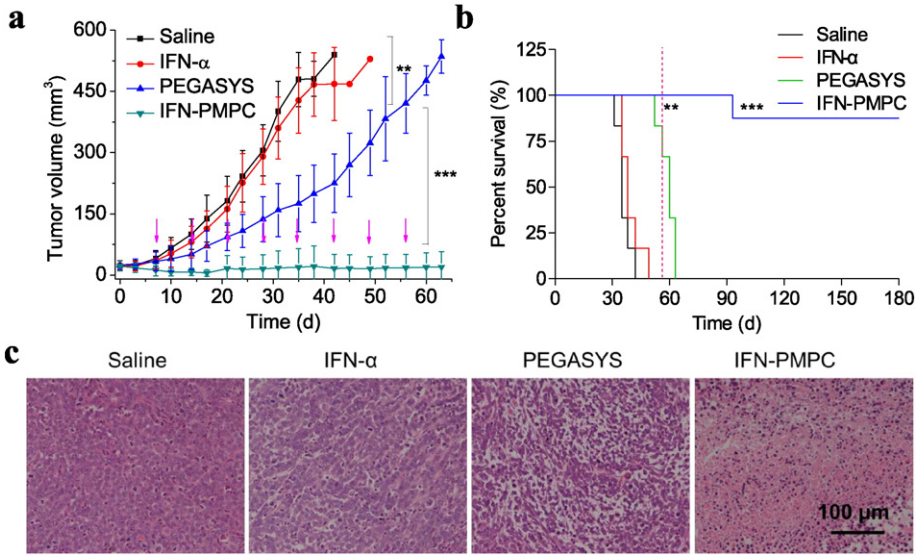

Fig. 4. Antitumor efficacy of IFN-PMPC. (a) Inhibition of tumor growth. Mice were weekly treated with saline, IFN-α, PEGASYS, or IFN-PMPC. The arrows indicate the time of dosing. (b) Cumulative survival of mice. The vertical line indicates the end of treatment. Data are shown as mean ± S.D. (n = 6–8, $^{**}P < 0.01$ for PEGASYS *versus* IFN-α, $^{***}P < 0.001$ for IFN-PMPC *versus* PEGASYS). (c) H&E staining of tumor tissues of mice at 21 days post treatment.

PEGASYS or IFN-PMPC appeared to be normal as compared with those of saline treated mice (Fig. S10), indicating that these treatments did not cause appreciable hematological toxicity. Overall, these results show that IFN-PMPC treatment is safe in systemic toxicity, which, at the same dose, is comparable to IFN-α and PEGASYS treatments.

4. Conclusions

In conclusion, we show SIG of PMPC at the C-terminus of IFN-α to yield a site-specific (C-terminal) and stoichiometric (1:1) IFN-PMPC conjugate and a head-to-head comparison of the PMPC conjugate with IFN-α and PEGASYS in cancer therapy. Such a direct comparison study leads to several findings that are interesting for the development of next-generation protein therapeutics. The molecular weight (57 kDa) of PMPC of the IFN-PMPC conjugate is 1.4-fold higher than that (40 kDa) of branced PEG of PEGASYS. However, the IFN-PMPC conjugate just possesses one polymer chain at the C-terminus of IFN that is far away from the receptor binding sites [30,31], whereas PEGASYS has more than one polymer chains at diverse positions that may be close to or be the receptor binding sites of the protein [8,9]. The structural distinctions between IFN-PMPC and PEGASYS directly lead to two findings that are responsive for the improved anticancer efficacy of IFN-PMPC over PEGASYS: (1) the *in vitro* antiproliferative activity of IFN-PMPC is 8.7-fold higher than that of PEGASYS; and (2) the pharmacokinetics and biodistribution properties of IFN-PMPC are comparable to those of PEGASYS. Additionally, PMPC is a biomimetic and zwitterionic polymer [25–28], which may be more biocompatible than PEG that is somewhat immunogenic [11–13]. The IFN-PMPC conjugate is also better than the IFN-POEGMA conjugate with the similar polymer molecular weight of *ca.* 60 kDa in *in vitro* bioactivity, and *in vivo* pharmacokinetics, biodistribution and antitumor efficacy [24]. The polymer molecular weight dependence of the protein funtion will be investigated in future study. This combination of features makes PMPC conjugates prepared by SIG interesting as a new and general platform for the delivery of other therapeutically important peptides and proteins with short circulating half-lives, such as interferon beta/gamma/lambda (IFN-β/γ/λ), erythropoietin (EPO), interleukin-22 (IL-22), granulocyte colony-stimulating factor (G-CSF), epidermal growth factor (EGF), insulin-like growth factor (IGF) and glucagon-like peptide-1 (GLP-1). This technology may accelerate the development of more and better long-lived protein/peptide drugs for the treatment of a variety of diseases.

Acknowledgements

This study was financially supported by Grants from National Natural Science Foundation of China (Grant No. 21274043, 21534006 to W. G.). We thank Dr. Zai Chang and Dr. Zhongchen Xie for assistance in animal study, Prof. Haiteng Deng and Technician Yan Gao for MS analysis of protein sample.

Appendix A. Supplementary data

Supplementary data (Fig. S1–Fig. S10 and Table S1) related to this article can be found at http://dx.doi.org/10.1016/j.jconrel.2016.07.007.

References

[1] S. Elliott, T. Lorenzini, S. Asher, K. Aoki, D. Brankow, L. Buck, L. Busse, D. Chang, J. Fuller, J. Grant, N. Hernday, M. Hokum, S. Hu, A. Knudten, N. Levin, R. Komorowski, F. Martin, R. Navarro, T. Osslund, G. Rogers, N. Rogers, G. Trail, J. Egrie, Enhancement of therapeutic protein in vivo activities through glycoengineering, Nat. Biotechnol. 21 (2003) 414–421.
[2] W. Zhao, F. Liu, Y. Chen, J. Bai, W. Gao, Synthesis of well-defined protein-polymer conjugates for biomedicine, Polymer 66 (2015) A1–A10.
[3] B. Leader, Q.J. Baca, D.E. Golan, Protein therapeutics: a summary and pharmacological classification, Nat. Rev. Drug Discov. 7 (2008) 21–39.
[4] J.M. Harris, R.B. Chess, Effect of PEGylation on pharmaceuticals, Nat. Rev. Drug Discov. 2 (2003) 214–221.
[5] B.K. Lee, J.S. Kwon, H.J. Kim, S. Yamamoto, E.K. Lee, Solid-phase PEGylation of recombinant interferon α-2a for site-specific modification: process performance, characterization, and in vitro bioactivity, Bioconjug. Chem. 18 (2007) 1728–1734.
[6] K.R. Reddy, M.W. Modi, S. Pedder, Use of peginterferon alfa-2a (40 KD) (Pegasys®) for the treatment of hepatitis C, Adv. Drug Deliv. Rev. 54 (2002) 571–586.
[7] Y.S. Wang, S. Youngster, M. Grace, J. Bausch, R. Bordens, D.F. Wyss, Structural and biological characterization of pegylated recombinant interferon alpha-2b and its therapeutic implications, Adv. Drug Deliv. Rev. 54 (2002) 547–570.
[8] F.M. Veronese, Peptide and protein PEGylation: a review of problems and solutions, Biomaterials 22 (2001) 405–417.
[9] J.E. Seely, C.W. Richey, Use of ion-exchange chromatography and hydrophobic interaction chromatography in the preparation and recovery of polyethylene glycol-linked proteins, J. Chromatogr. A 908 (2001) 235–241.
[10] S. Shaunak, A. Godwin, J.W. Choi, S. Balan, E. Pedone, D. Vijayarangam, S. Heidelberger, I. Teo, M. Zloh, S. Brocchini, Site-specific PEGylation of native disulfide bonds in therapeutic proteins, Nat. Chem. Biol. 2 (2006) 312–313.
[11] K. Knop, R. Hoogenboom, D. Fischer, U.S. Schubert, Poly (ethylene glycol) in drug delivery: pros and cons as well as potential alternatives, Angew. Chem. Int. Ed. 49 (2010) 6288–6308.
[12] G. Pasut, M. Sergi, F.M. Veronese, Anti-cancer PEG-enzymes: 30 years old, but still a current approach, Adv. Drug Deliv. Rev. 60 (2008) 69–78.

[13] K. Środa, J. Rydlewski, M. Langner, A. Kozubek, M. Grzybek, A.F. Sikorski, Repeated injections of PEG-PE liposomes generate anti-PEG antibodies, Cell. Mol. Biol. 10 (2005) 37–47.
[14] S. Bhattacharjee, W. Liu, W.H. Wang, I. Weitzhandler, X. Li, Y. Qi, J. Liu, Y. Pang, D.F. Hunt, A. Chilkoti, Site-specific zwitterionic polymer conjugates of a protein have long plasma circulation, ChemBioChem 16 (2015) 2451–2455.
[15] R. Falatach, S. Li, S. Sloane, C. Mcglone, J.A. Berberich, R.C. Page, S. Averick, D. Konkolewicz, Why synthesize protein–polymer conjugates? The stability and activity of chymotrypsin-polymer bioconjugates synthesized by RAFT, Polymer 72 (2015) 382–386.
[16] J. Zhang, J. Du, M. Yan, A. Dhaliwal, J. Wen, F. Liu, T. Segura, Y. Lu, Synthesis of protein nano-conjugates for cancer therapy, Nano Res. 4 (2011) 425–433.
[17] V. Depp, A. Alikhani, V. Grammer, B.S. Lele, Native protein-initiated ATRP: a viable and potentially superior alternative to PEGylation for stabilizing biologics, Acta Biomater. 5 (2009) 560–569.
[18] K.L. Heredia, D. Bontempo, T. Ly, J.T. Byers, S. Halstenberg, H.D. Maynard, In situ preparation of protein-"smart" polymer conjugates with retention of bioactivity, J. Am. Chem. Soc. 127 (2005) 16955–16960.
[19] B.S. Lele, H. Murata, K. Matyjaszewski, A.J. Russell, Synthesis of uniform protein-polymer conjugates, Biomacromolecules 6 (2005) 3380–3387.
[20] J.C. Peeler, B.F. Woodman, S. Averick, S.J. Miyake-Stoner, A.L. Stokes, K.R. Hess, K. Matyjaszewski, R.A. Mehl, Genetically encoded initiator for polymer growth from proteins, J. Am. Chem. Soc. 132 (2010) 13575–13577.
[21] S. Averick, A. Simakova, S. Park, D. Konkolewicz, A.J.D. Magenau, R.A. Mehl, K. Matyjaszewski, ATRP under biologically relevant conditions: grafting from a protein, ACS Macro Lett. 1 (2012) 6–10.
[22] W. Gao, W. Liu, J.A. Mackay, M.R. Zalutsky, E.J. Toone, A. Chilkoti, In situ growth of a stoichiometric PEG-like conjugate at a protein's N-terminus with significantly improved pharmacokinetics, Proc. Natl. Acad. Sci. U. S. A. 106 (2009) 15231–152316.
[23] W. Gao, W. Liu, T. Christensen, M.R. Zalutsky, A. Chilkoti, In situ growth of a PEG-like polymer from the C terminus of an intein fusion protein improves pharmacokinetics and tumor accumulation, Proc. Natl. Acad. Sci. U. S. A. 107 (2010) 16432–16437.
[24] J. Hu, G. Wang, W. Zhao, X. Liu, L. Zhang, W. Gao, Site-specific in situ growth of an interferon-polymer conjugate that outperforms PEGASYS in cancer therapy, Biomaterials 96 (2016) 84–92.
[25] K. Ishihara, N. Nakabayashi, K. Fukumoto, J. Aoki, Improvement of blood compatibility on cellulose dialysis membrane I. Grafting of 2-methacryloyloxyethyl phosphorylcholine on to a cellulose membrane surface, Biomaterials 13 (1992) 235–239.
[26] H. Yumoto, K. Hirota, K. Hirao, T. Miyazaki, N. Yamamoto, K. Miyamoto, K. Murakami, N. Fujiwara, T. Matsuo, Y. Miyake, Anti-inflammatory and protective effects of 2-methacryloyloxyethyl phosphorylcholine polymer on oral epithelial cells, J. Biomed. Mater. Res. A 103 (2015) 555–563.
[27] K. Ishihara, H. Nomura, T. Mihara, K. Kurita, Y. Iwasaki, N. Nakabayashi, Why do phospholipid polymers reduce protein adsorption? J. Biomed. Mater. Res. 39 (1998) 323–330.
[28] K. Hirota, H. Yumoto, K. Miyamoto, N. Yamamoto, K. Murakami, Y. Hoshino, T. Matsuo, Y. Miyake, MPC-polymer reduces adherence and biofilm formation by oral bacteria, J. Dent. Res. 90 (2011) 900–905.
[29] A. Lewis, Y. Tang, S. Brocchini, J. Choi, A. Godwin, Poly (2-methacryloyloxyethyl phosphorylcholine) for protein conjugation, Bioconjug. Chem. 19 (2008) 2144–2155.
[30] W. Klaus, B. Gsell, A.M. Labhardt, B. Wipf, H. Senn, The three-dimensional high resolution structure of human interferon α-2a determined by heteronuclear NMR spectroscopy in solution, J. Mol. Biol. 274 (1997) 661–675.
[31] J. Hu, G. Wang, X. Liu, W. Gao, Enhancing pharmacokinetics, tumor accumulation and antitumor efficacy by elastin-like polypeptide fusion of interferon alpha, Adv. Mater. 27 (2015) 7320–7324.
[32] L.M. Pfeffer, C.A. Dinarello, R.B. Herberman, B.R. Williams, E.C. Borden, R. Bordens, M.R. Walter, T.L. Nagabhushan, P.P. Trotta, S. Pestka, Biological properties of recombinant α-interferons: 40th anniversary of the discovery of interferons, Cancer Res. 58 (1998) 2489–2499.